2 − 3. Cytotoxicity test (Colony formation assay)

CHL cells were seeded at 50/well in 24-well plates. After 24-h incubation, they were treated with a test chemical or vehicle control for six days. The colonies formed were fixed with methanol and stained with 3% Giemsa solution. The number of colonies on each well was counted, and the relative survival was calculated based on comparison with the control colonies. The cytotoxic potential of the chemical was expressed as the concentration at which the relative survival was 50% of control (IC_{50}). The IC_{50} value was calculated by the probit method.

2 − 4. Chromosome aberration (CA) test

Cells were seeded at 1.5 x 10^5/plate (60 mm in diameter) and incubated at 37°C for 17 h. They were then treated with a test chemical for 24 or 48 h, and colcemid (0.2 μg/ml) was added for the final 2 h. For metabolic activation, cells were treated with a test chemical for 6 h in the presence or absence of S9 mix[3] (Kikkoman, Noda, Japan) and cultured with fresh medium for another 18 h with colcemid added for the last 2 h. The S9 fraction was prepared from the livers of Sprague-Dawley rats pretreated with phenobarbital and 5,6-benzoflavone. The final concentration of the S9 fraction was 5 v/v%. Chromosome preparations were made as reported previously[4]. All slides were coded, and the number of cells with structural CAs was counted for 100 well-spread metaphases with a modal chromosome number of 25 ± 2. The number of cells with numerical CAs was counted on 100 metaphases. In our historical database[4], the frequency of CHL cells with structural CAs or polyploidy in both untreated and solvent-treated negative controls did not exceed 4%. The experimental groups were judged as negative if the total CA frequency was less than 5.0%, inconclusive if it was 5.0 to up to 10.0%, and positive if it was 10.0% or more. The number of mitotic cells was counted for 1000 cells. Relative mitotic index was calculated based on comparison with the number of mitotic cells in controls to show the concurrent cytotoxicity. Solvent − treated cells served as the negative control. Experiments were performed twice, and representative data are shown.

2 − 5. Micronucleus (MN) test

CHL cells were seeded and incubated as they were in the CA test, treated with a chemical for 24 or 48 h in the absence of S9 mix (because there was no effect in its presence in the CA test), and harvested immediately. MN preparations were made as reported previously[5]. The cells were stained by mounting in 40 μg/ml acridine orange in phosphate-buffered saline (PBS) and were immediately observed at 400 x magnification by fluorescence microscopy with a model Nikon Eclipse E600 and a B-2A filter block. All slides were coded, and they were observed and judged as reported previously[6]. Briefly, the number of MN cells among 1000 intact interphase cells was counted. Cells with a main nucleus and a single MN were categorized into two groups: those with a MN whose diameter was less than one-third of the main nucleus and those with a MN whose diameter was one-third to one half the diameter of the main nucleus. A cell with two or more MN was recorded as a multi MN cell. In addition, we examined 1000 total cells and scored polynuclear (PN) cells, including polynuclear cells, karyorrhectic cells, and binucleates, and mitotic (M) cells. Experiments were performed twice and representative data are shown. We analyzed the data using a χ^2-test for treated versus control groups.

3. Results

Fibers of CMBA precipitated in the culture medium are shown in Fig. 2. Single and bundled fibers are shown ranging from around 2 to 33 μm in length.

Chrysotile B, with an IC_{50} of 0.398 μg/ml was much more cytotoxic than CMBA, with an IC_{50} of 11.0 μg/ml

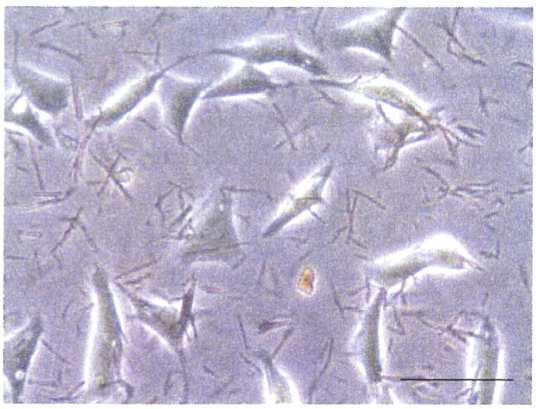

Fig. 2 Phase contrast micrograph of fibers of CMBA precipitated in the culture medium after its DMSO solution was added
Single and bundled fibers are shown ranging the length from around 2 to 33 μm. Bar indicates 50 μm.

(Fig. 3). As fiber concentrations are typically given in $\mu g/cm^2$, those in $\mu g/cm^2$ are added in parentheses for chrysotile B in graphs and a table.

To show the fiber length of CMBA and chrysotile B quantitatively, we measured them as follows: their suspension in the culture medium was placed on a glass microscope slide, covered with a cover slip, and then photographed under a light microscope. Length of fibers was measured on the enlarged photo prints. The fiber length distribution of CMBA and chrysotile B is shown in Fig. 4. CMBA and chrysotile B showed different distribution patterns. The fiber length distribution of CMBA spread broadly mainly from 3 to 15 μm. 77% of the fibers was shorter than or equal to 15 μm. On the other hand, chrysotile B showed a distribution with a peak at 1 μm and 85% of the fibers was shorter than or equal to 5 μm. In this connection, Timbrell reported that 97% of the fibers of the UICC chrysotile B was shorter than or equal to 5 μm[7].

In the CA test, CMBA induced polyploidy after 6-, 24-, and 48-h treatment without S9 mix in a concentration-dependent manner (Table 1). The concurrent cytotoxicity under the conditions was not strong as shown by the relative mitotic index. CMBA did not induce structural CAs under any experimental conditions. CMBA did not induce CAs at concentrations lower than 6.25 $\mu g/ml$.

Chrysotile B, on the other hand, induced polyploidy

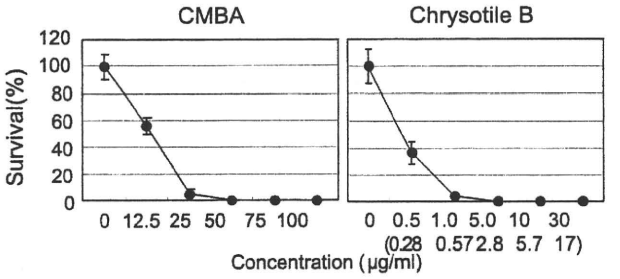

Fig. 3 Cytotoxicity of CMBA and chrysotile B
Values are expressed as mean ± SD for four wells. Figures in a parenthesis indicate concentrations in $\mu g/cm^2$.

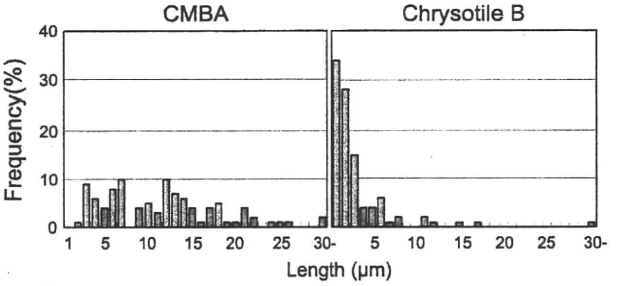

Fig. 4 Fiber length distribution of CMBA and chrysotile B
The average length of CMBA fibers was 10.95 μm.

Table 1 Chromosome aberration test of CMBA

T-R[a] (h)	S9 mix	Concentraton ($\mu g/ml$)	polyploid cells (%)	Cells with chromosome aberrtion[b] (%)							Relative mitotic index (%)
				ctg	ctb	cte	f	osb	cse	Total	
6 - 18	−	0	2	1	0	0	0	0	0	1	100
		20	12	0	0	0	0	1	0	1	127
		40	15	0	1	2	0	1	0	4	104
		60	25	2	1	0	0	0	0	3	80.0
		80	10	0	1	1	0	0	0	2	92.0
6 - 18	+	0	0	1	0	0	0	1	0	2	100
		20	1	1	0	1	0	0	0	2	85.6
		40	4	1	0	0	0	0	1	2	97.5
		60	3	1	0	1	0	0	1	3	99.2
		80	3	1	1	1	0	0	0	3	105
24 - 0	−	0	0	0	1	0	0	0	1	2	100
		6.25	1	0	0	0	0	0	0	0	137
		12.5	12	2	1	1	0	0	0	4	159
		25	26	0	0	0	0	0	0	0	123
		50	23	0	1	0	0	0	0	1	105
48 - 0	−	0	2	0	0	0	0	0	0	0	100
		6.25	1	0	0	0	0	0	0	0	71.2
		12.5	16	1	0	0	0	0	0	1	48.1
		25	46	0	0	0	0	0	0	0	65.4
		50	40	0	0	0	0	0	0	0	59.6

[a]Treatment and recovery time. [b]ctg, chromatid and chromosome gaps; ctb, chromatid breaks; cte, chromatid exchanges; f, fragmentation; csb, chromosome breaks; cse, chromosome exchanges.

under all the experimental conditions (Table 2). The lowest concentrations that induced polyploidy were ten times higher in the presence of S9 mix than its absence. Chrysotile B induced structural CAs, but at a low frequency.

We observed bi-, tri-, tetra-, and hexa-nuclear cells in MN preparations after treatment with CMBA (Fig. 5) and after treatment with chrysotile B (data not shown).

CMBA induced a small but statistically significant increase in the frequency of MN cells after 24- and 48-h treatments (Fig. 6). Surprisingly, the frequency of PN cells induced was about 50 times the control value. Binucleates were prominent at both 24- and 48-h, after which the ratio of polynuclear cells among the PN cells increased. CMBA did not significantly increase the frequency of M cells.

Chrysotile B induced the similar pattern of MN, PN, and M cells as CMBA (Fig. 7). The only difference from CMBA in the MN test was the concentrations tested.

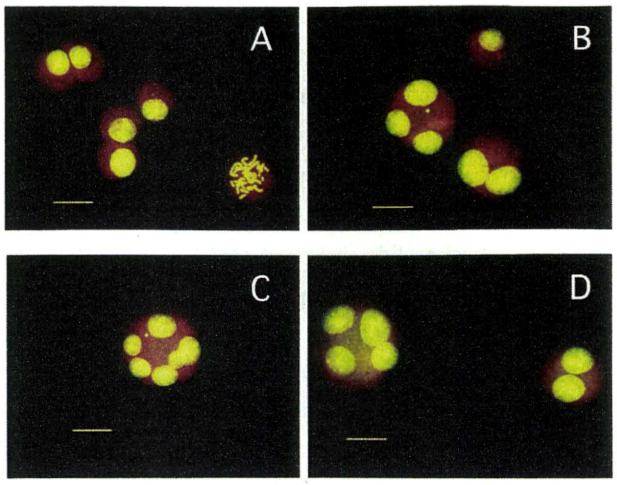

Fig. 5 CHL cells treated with CMBA in MN preparations A, intact interphase cells and a mitotic cell observed in control. B and C, A binucleate, a tri-nuclear cell with an MN, and a hexa-nuclear cell with a MN observed after treatment with CMBA at 20 μg/ml for 48 h. D, a binucleate and a tetra-nuclear cell observed after treatment with CMBA at 40 μg/ml for 48 h. MN preparations were stained with acridine orange. Yellow indicates nuclei and chromosomes and red indicates cytoplasm. Bar represents 20 μm.

Table 2 Chromosome aberration test of chrysotile B

T-R[a] (h)	S9 mix	Concentraton (μg/ml)	Concentraton (μg/cm^2)	polyploid cells (%)	Cells with chromosome aberrtion[b] (%) ctg	ctb	cte	f	osb	cse	Total	Relative mitotic index (%)
6 - 18	−	0	0	1	0	0	0	0	0	0	0	100
		0.5	0.12	7	0	0	0	0	0	0	0	88.9
		1	0.25	13	1	0	0	0	0	0	1	87.8
		5	1.2	28	2	2	1	0	1	1	7	82.2
		10	2.5	44	2	2	2	0	3	0	6	62.2
		30	7.4	29	0	2	0	0	0	0	2	51.1
		50	12	20	0	0	0	0	2	0	2	42.2
6 - 18	+	0	0	1	1	1	2	0	0	0	3	100
		0.5	0.12	0	0	0	0	0	0	0	0	101
		1	0.25	2	1	0	0	0	0	1	2	120
		5	1.2	4	0	0	0	0	0	0	0	117
		10	2.5	10	1	1	0	0	0	1	3	108
		30	7.4	11	1	1	2	0	0	0	3	93.5
		50	12	15	0	0	1	0	1	0	2	79.2
24 - 0	−	0	0	2	1	0	0	0	0	0	1	100
		0.5	0.12	7	2	0	0	0	1	0	3	138
		1	0.25	10	1	2	2	0	2	0	5	117
		5	1.2	25	0	0	0	0	0	0	0	72.1
		10	2.5	32	0	0	0	0	2	0	2	74.4
		30	7.4								Tox	
48 - 0	−	0	0	1	0	0	0	0	0	0	0	100
		0.5	0.12	9	0	1	0	0	0	0	1	93.0
		1	0.25	15	5	2	1	0	2	1	7	144
		5	1.2	39	0	1	0	1	0	2	3	126
		10	2.5	30	3	7	4	0	4	1	11	86.0
		30	7.4								Tox	

[a, b] See the footnote in Table 1. Tox; cells were killed.

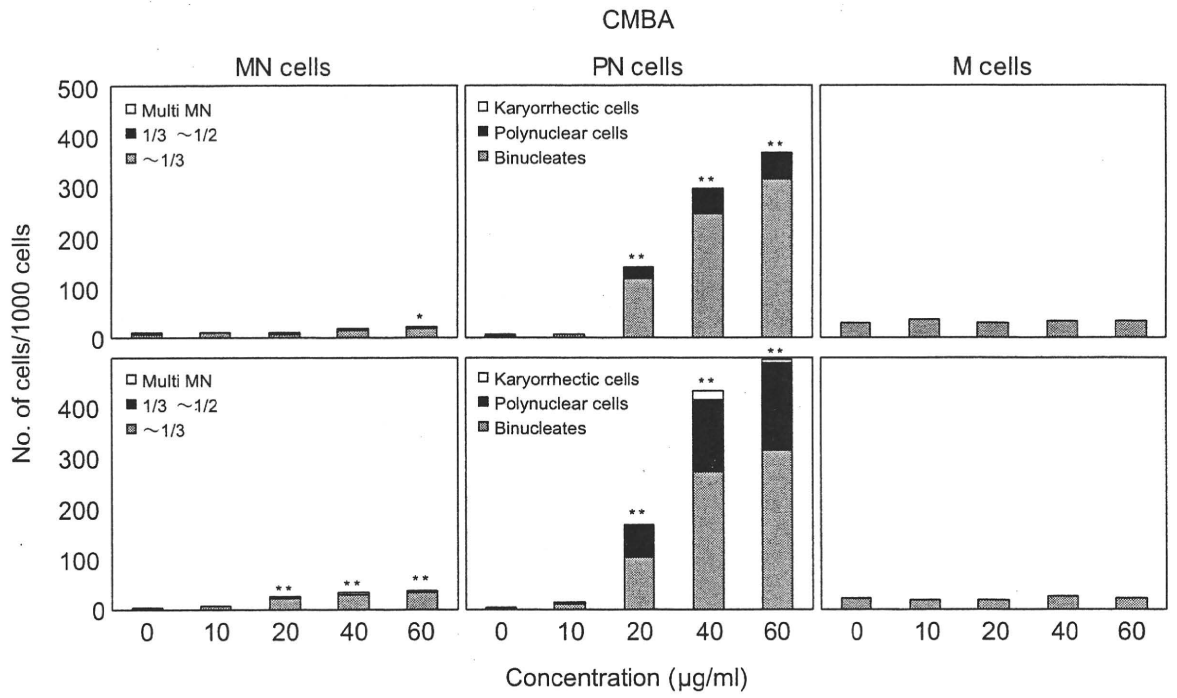

Fig. 6 Results of the *in vitro* MN test with CMBA for 24 h (top) and 48 h (bottom)
The left graphs show the number of MN cells/1000 intact interphase cells. The middle graphs show the number of PN cells/1000 total cells, including binucleates, polynuclear cells, and karyorrhectic cells. The right graphs show the number of M cells/1000 total cells. $^{*}P < 0.05$, $^{**}P < 0.01$.

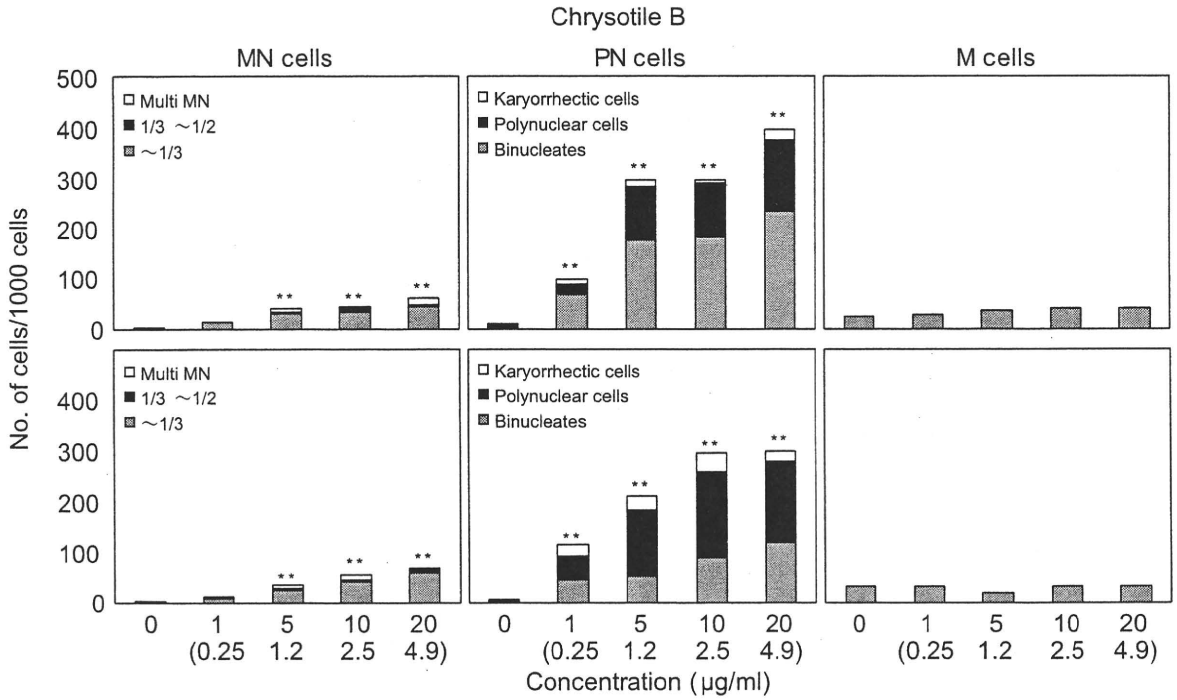

Fig. 7 Results of the *in vitro* MN test of chrysotile B
See legend to Fig. 6. Figures in parentheses indicate concentrations in $\mu g/cm^2$.

4. Discussion

We found that CMBA and chrysotile B showed a similar induction pattern of MN, PN, and M cells in the MN test, and both induced polyploidy in a similar manner in the CA test, although their fiber length distribution was different from each other strictly speaking. Koshi et al.[8] reported that a size-selected sample (81% of fibers was less than 5 μm long) of

UICC chrysotile B induced 34% polyploidy at 10 μg/ml after 46-h treatment. Our result was consistent well with theirs.

In a previous study[6], we showed that clastogens can be distinguished from aneugens in the MN test according to their induction pattern of MN, PN, and M cells. Aneugens were always accompanied by a high frequency of M cells. Vincristine induced a high frequency of MN and M cells in addition to the induction of PN cells. CMBA and chrysotile B, however, were clearly aneugens, but they did not induce M cells. We can estimate that the mechanism of polyploidy induction by CMBA may be different from that of vincristine.

We experienced a similar response of binucleate induction by 2-phenylbenzotriazole－type water pollutant (PBTA-2), which has cytochalasin B (Cyt B) -mimetic activity[9]. At first CMBA seemed to be similar to PBTA-2 in its induction pattern of MN, PN, and M cells in the MN test. But, CMBA was different from PBTA-2 in polyploidy induction in the CA test. PBTA-2 induced 12% polyploidy at most only at a highest concentration of 100 μg/ml. On the other hand, CMBA induced polyploidy in a concentration-dependent manner with an example of 46% at 25 μg/ml. Chrysotile B also induced polyploidy in a concentration-dependent manner with an example of 44% at 10 μg/ml.

One mechanism for the formation of bi- and multinucleated cells is attributed to hydrophobicity[10]. Chrysotile B is a mineral, so that was not the case. Inhibition of actin polymerization could be a mechanism. If so, formation of contractile rings would be inhibited resulting in no cleavage furrows at telophase, but we could observe cleavage furrows after CMBA treatment, even at 40 μg/ml (data not shown). Crocidolite fibers block cytokinesis but not cleavage furrows[11] and that could lead to binucleates. That might also be the case for CMBA. Needle crystals of vitamin B_2 induce polyploidy (32% at 150 μg/ml) in CHL/IU cells[12], apparently by physically fixing the cell shape and thereby preventing normal mitosis. This mechanism seems to be similar to that of the paper above[11].

In the present study, the uptake of fibers into cells was not investigated. Internalization of fibers is considered to play an important role in their cytotoxic and genotoxic effects. Further studies are needed to substantiate the findings in the present study and to understand the mechanism of polyploidy and binucleates induction mentioned above.

In the practical use of CMBA, it is commercially available as a water solution for textile dyeing. That suggests that there may be a very low possibility for us to be exposed to fibers of CMBA in the dyeing industry. CMBA should be handled carefully when manufactured in a factory.

References

1) Koyama, H., Utakoji, T. and Ono, T.: *Gann* **61**, 161-167 (1970)
2) Ishidate, M. Jr. and Odashima, S.: *Mutat. Res.*, **48**, 337-354 (1977)
3) Matsuoka, A., Hayashi, M. and Ishidate, M. Jr.: *Mutat. Res.*, **66**, 277-290 (1979)
4) Matsuoka, A., Sofuni, T., Miyata, N. and Ishidate, M. Jr.: *Mutat. Res.*, **259**, 103-110 (1991)
5) Matsuoka, A., Yamazaki, N., Suzuki, T., Hayashi, M. and Sofuni, T.: *Mutat. Res.*, **272**, 223-236 (1993)
6) Matsuoka, A., Matsuura, K., Sakamoto, H., Hayashi, M. and Sofuni, T.: *Mutagenesis*, **14**, 385-389 (1999)
7) Timbrell, V.: Pneumoconiosis, Proc. Inter. Conf. Johannesburg, eds. by Shapiro, H.A., pp. 28-36 (1969)
8) Koshi, K., Kohyama, N., Myojo, T. and Fukuda, K.: *Ind. Health*, **29**, 37-5 (1991)
9) Matsuoka, A., Sakamoto, H., Tadokoro, S., Tada, A., Terao, Y., Nukaya, H. and Wakabayashi, K.: *Mutat. Res.*, **464**, 161-167 (2000)
10) Schultz, N. and Öfelt, A.: *Chem.-Biol. Interactions*, **126**, 97-123 (2000)
11) Jensen, G.G., Jensen, L.C.W., Rieder, C.L., Cole, R.W. and Ault, J.G.: *Carcinogenesis*, **17**, 2013-2021 (1996)
12) Kawaguchi, Y., Hayashi, H., Sato, M. and Shindo, Y.: *Mutat. Res.*, **371**, 1-7 (1997)

Bull. Natl. Inst. Health Sci., **128**, 50-57 (2010) **Original**

*In vitro*培養ヒト間葉系幹細胞の細胞遺伝学的安全性評価法に関する研究

松岡厚子

Cytogenetic study on safety evaluation of human mesenchymal stem cells cultured *in vitro*

Atsuko Matsuoka

Human mesenchymal stem cells (hMSCs) are one of the promising sources for regenerative medicine. In general, hMSCs are supposed to grow indefinitely and differentiate to various kinds of cells. The indefinite growth is concerned due to its misleading to carcinogenesis in the practical use of hMSCs in regenerative medicine. In the present study, we investigated unexpected changes, especially in genetic aspect, in hMSCs during culture utilizing fluorescence *in situ* hybridization (FISH) with chromosome specific DNA probes for chromosomes 1 and 4, or a locus specific identifier for *c-myc*. Three lots of hMSCs and three human cancer cell lines (HeLa S3, HOS and OUMS-27) were analyzed. The results of this study suggest that both observation of cell morphology and FISH analysis of *c-myc* aberrant cells in interphase cells are useful for evaluating safety of hMSCs expanded *in vitro*.

Keywords: human mesenchymal stem cells, *c-myc*, FISH, *in vitro* safety evaluation

1．はじめに

ヒト間葉系幹細胞は，骨，軟骨，筋，腱，脂肪等の組織への分化が可能であるため，再生医療分野で，従来治療法がなかった疾患への応用が期待されている．事故や病気で失った組織の修復，再建が，形態的にだけでなく機能的にも可能であればまさに夢のような治療法である．しかし，一般に幹細胞は分化能と共に無限増殖能を有しており，再生組織としてある程度の量まで増殖させてヒト体内へ移植できるという利点と，両機能を体内で適切に制御できるかという問題点を含んでいる．本研究では，再生医療において*in vitro*で培養中に幹細胞が目的以外の形質をもった細胞に変化しないこと，特に遺伝的形質に変化がないことを確認し，患者に戻される細胞の安全性を担保する方法を検討した．

2．方法

2－1　細胞

市販のヒト骨髄由来間葉系幹細胞（human mesenchymal stem cells; hMSC）3ロットをCambrex社（米国）より購入した（Table 1）．また，hMSCが増殖に異常をきたした極端な例として癌を想定し，3種の癌細胞株（Table 1）の検討を行なった．癌細胞株としては，制癌剤スクリーニングに繁用されるHeLa S3細胞，hMSCから分化誘導可能な組織である骨及び軟骨に生じた癌由来の細胞株，それぞれHOS及びOUMS-27の計3種を用いた．hMSCはCambrex社製の専用培地を，また，癌細胞株の培養は添付文書で推奨されている培地を用いた．

2－2　増殖

3ロットのhMSCを同じ条件で継代し，定期的にサン

Table 1　List of cells used

Normal human mesenchymal stem cells

Lot	Origin	Donor
hMSC 10796	bone marrow	26 Y, male, Black
hMSC 10909	bone marrow	19 Y, female, Black
hMSC 11809	bone marrow	21 Y, male, Other

Human cancer cell lines

Cell line	Supplier	Origin	Donor
HeLa S3	JCRB*	Cervical cancer	31 Y, female
HOS	Dainippon**	Osteosarcoma	13 Y, female, Caucasian
OUMS-27	JCRB	Chondrosarcoma	65 Y, male

hMSC: human mesenchymal stem cells, *Health Science Research Resources Bank, **Dainippon Pharmaceutical.

To whom correspondence should be addressed:
Atsuko Matsuoka; 1-18-1 Kamiyoga, Setagaya-ku, Tokyo 158-8501, Japan; Tel: +81-3-3700-9268; Fax: +81-3-3707-6950; E-mail: matsuoka@nihs.go.jp

プリングし，一定数の細胞播種後，経時的にトリプシンで細胞を剥離し，血球計算盤で細胞数を計数した．各測定点につき3枚のプレートを用い，その平均値を増殖曲線にプロットした．癌細胞株HeLa S3についても同様に増殖曲線を作成した．

2－3　老化細胞染色

細胞が老化に伴い，pH 6.0で検出できるβ-galactosidase (Senescence associated β- galactosidase, SA-β-Gal) 活性を示すことを利用した染色法[1]で，Senescence Detection Kit (Oncogene, Cat# QIA117) を用いて染色した．老化細胞は青く染まる．

2－4　染色体解析

染色体異常解析には，従来の分染法より簡便に実施できる蛍光 *in situ* ハイビリダイゼーション (fluorescence *in situ* hybridization; FISH) 法を採用した．

hMSCの染色体標本は以下のように作製した．コルセミド (0.02 μg/ml) で一晩処理し，トリプシンで細胞を回収した．75 mM塩化カリウム溶液で室温20分間低張処理したのち，カルノア液 (氷酢酸：メタノール＝1：3混液) で3回固定した．細胞懸濁液をスライドグラスに滴下し，自然乾燥させた．癌細胞株の染色体標本は，コルセミド (0.1-0.2 μg/ml) で2－4時間処理した以外は，hMSCと同様に作製した．

染色体数計数用の標本はギムザ染色し，FISH解析用標本はDNAプローブのハイブリダイゼーションを行うまで，窒素ガスを封入したビニル袋に密閉し，－20℃に保管した．

FISH解析は，1番染色体，4番染色体及び*c-myc*のDNAプローブ (SpectrumOrange標識, VYSIS社，米国) を用いた．前2者は染色体の構造異常を解析する目的で，ハイブリにより比較的明るいシグナルが観察されるため観察が容易であり，また，比較的大きな染色体であるため効率よく構造異常を検出できると考えて選択した．*c-myc*は正常では8番染色体の長腕の先端 (8q24.12-q24.13) にシグナルが観察されるが，プローブ長が短い (約120 kb) ため間期細胞でもシグナルの正確な観察ができるという利点があり，ヒト癌組織においてしばしば観察される増幅を観察できると考え選択した．増幅は癌遺伝子の過剰発現の一つの機序と考えられている．

プローブDNAを70℃で5分間熱変性させ，すぐに氷冷した．染色体DNAを変性させるために，スライドグラスを70℃の70%フォルムアミド溶液に4分間浸し，すぐに，氷冷した70%エタノールに移し，その後続けて85%，100%エタノールに移し，自然乾燥させた．スライドグラスに熱変性したプローブDNA液をのせ，カバーグラスで覆い，回りをペーパーボンドでシール後，37℃で一晩ハイブリダイズさせた．ハイブリダイズ終了後，45℃の50%フォルムアミド液で3回，2 x SSC液で1回，0.1%NP-40を含む2 x SSC液で1回洗浄した．その後自然乾燥させて，DAPI Counterstain (VYSIS社) でマウントし，蛍光顕微鏡 (Nikon E600) で観察した[2]．間期細胞で観察される*c-myc*の見かけ上1個のシグナルは，G1期の細胞とG2期の細胞で実体は異なり，それぞれ，locus 1個とlocus 2個に相当する．

染色体数分布は，ギムザ染色した分裂中期像を撮影し，プリント上で染色体数を計数して作成した．hMSCは30本以上の，癌細胞株は43本以上の染色体を有する分裂中期像を計数対象とした．

3．結果

今回入手したhMSCはヒトから採取後最低2回の継代増殖を行い，その細胞を凍結した製品である．In vitro継代培養による影響を調べるためには，再生医療においては患者から採取直後の細胞と，患者へ戻される移植直前の細胞との比較を行う必要があると考えられる．本研究では，実施可能な範囲で，すなわち入手したhMSCを培養開始直後の細胞と複数回継代を繰り返した後の細胞との比較をもって，再生医療での上記比較に代えた．

3－1　増殖

hMSC 10796では，1代目では順調な増殖が認められたが，4代目，6代目では増殖が低下し，10代目（データ未掲載）では殆ど増殖しなかった (Fig. 1)．hMSC 10909では5代目までは順調な増殖を示し，10代目では増殖の低下が認められた．hMSC 11809の増殖は1代目

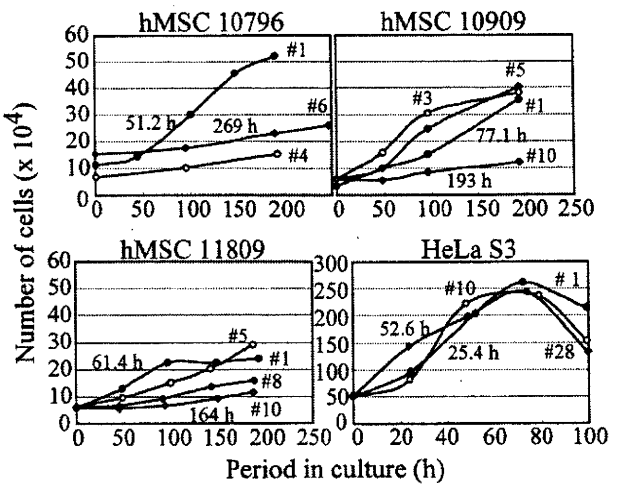

Fig. 1 Growth curve of three hMSCs and HeLa S3
The #number indicates the passage number. The doubling time for the first and the last passage is indicated in the graphs.

から低調で，増殖率測定時の培養100時間目までは，順調に増殖していたが，その後ほとんど増殖しなくなった．HeLa S3細胞では継代数にかかわらず一定の増殖を示し，倍加時間は平均約30時間であった．hMSCの増殖速度は継代とともに低下し，ロット差も認められるが，10代目以降はほとんど増殖しなくなった．

3－2　細胞形態及び老化細胞染色

hMSC 10909の老化細胞染色像（位相差顕微鏡像）をFig. 2に示す．培養開始直後（#1）は，細胞全体の配列に一定の流れが認められ，個々の細胞の形も細長い紡錘型で，青く染まる細胞はなかったが，培養後期（#7及び#13）には配列の配向性は低下し，個々の細胞は伸展，肥大し，細胞の中央部が青く染まった．しかし，継代がかなりすすんでも，すべての細胞が青く染色されることはなかった．一方，HeLa S3細胞では継代による形態変化は認められず，一部敷石状で大部分は球形の形態を維持した．28代目まで継代したが，青く染まる細胞は観察されなかった．

3－3　染色体解析

生命現象の基本である遺伝情報を担う染色体は，種によって数，形態が一定で，安定である．変化を起こしにくい染色体を対象とすればわずかな変化も検出し易いと考え，*in vitro*培養によるhMSCの安全性評価指標として検討した．

hMSC 10909の継代による染色体数分布の変化をFig. 3に示す．1，3，5代目での観察では，いずれもヒト正常染色体数46本にピークを示す分布を示し，継代による明らかな変化は認められなかった．

癌細胞株3種の結果をFig. 4に示す．HeLa S3細胞及びHOS細胞はそれぞれ，67本及び48本にピークを示す分布を示したが，OUMS-27細胞では目立ったピークはなく，69－78本を中心として幅広い分布を示した．

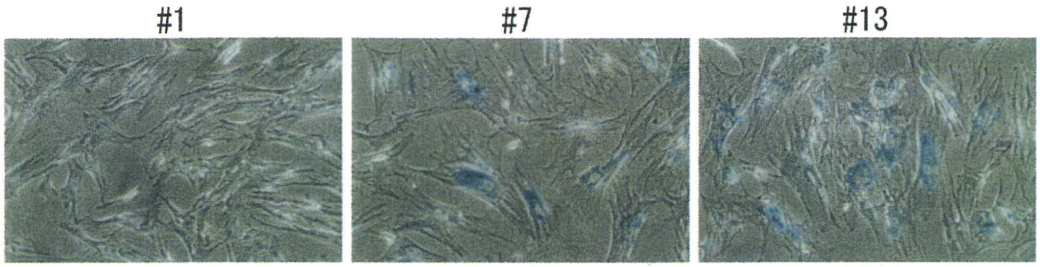

Fig. 2　Senescent cells observed in the hMSC culture (SA-β-Gal staining)
Although hMSC (10909) did not show senescent cells stained blue at early passage (#1), some of them changed to flat and big in shape and were stained blue in the center at middle (#7) and late passage (#13).

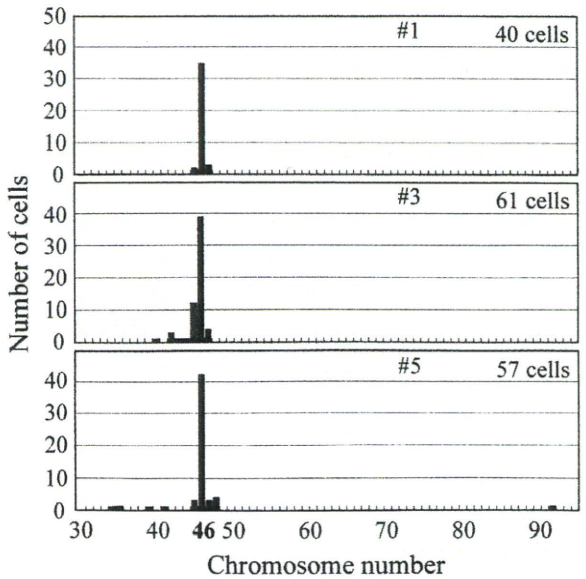

Fig. 3　Distribution of chromosome number of hMSC 10909 at the first, third and fifth passage
The number in the upper right corner indicates the number of cells analyzed.

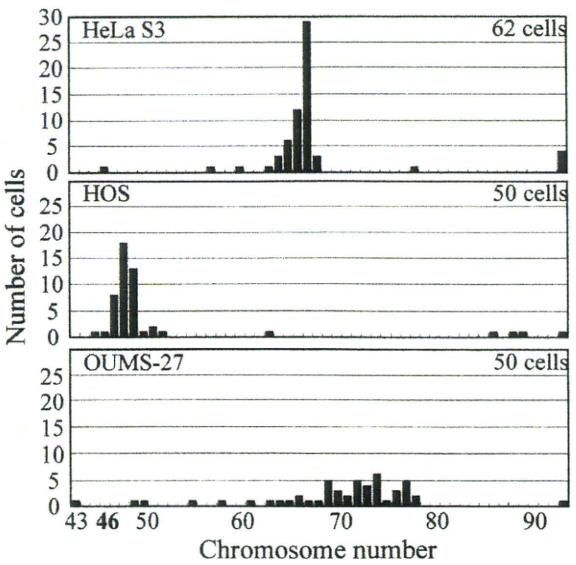

Fig. 4　Distribution of chromosome number of human cancer cell lines, HeLa S3, HOS and OUMS-27
The number in the upper right corner indicates the number of cells analyzed.

HeLa細胞は，継代10，28代目の解析も行なったが，染色体数分布に継代による変化は認められなかった．

3－3－1　ヒト癌細胞株でのFISH法による染色体異常解析

FISH法による染色体異常解析の有効性，癌の種類によって検出される異常頻度，型に特異性があるか，また解析プローブの特性を確認するため，増殖がよく観察細胞数も充分に得られ，高頻度の異常が予想される癌細胞を用いた解析を最初に行なった．

結果をTable 2に示す．いずれのプローブを使った解析でも，正常細胞では，1対の染色体の全部あるいは一部（*c-myc*）が染色され，2シグナルを示す．HeLa S3細胞では，1番染色体は100%の細胞で異常であったが，4番染色体での異常頻度は7%と低かった．

骨肉腫由来のHOS細胞では，1番，4番染色体とも全細胞で異常であった．1番染色体での異常をFig. 5 Bに，4番染色体での異常をFig. 5 Dに示す．

軟骨肉腫由来のOUMS-27細胞では，1番染色体では異常が100%の細胞で観察されたが，4番染色体では87%の細胞で正常な2シグナルが観察された．1番染色体の異常は，正常1番染色体が3本と転座1本（不完全型）（Fig. 5 C）の4シグナルからなる異常型が異常の半分を占めていた．

HeLa S3では，*c-myc*はほとんどの細胞で異常であった．HOS細胞では正常2シグナルを示す細胞が，分裂期細胞（染色体）の観察では61%，間期細胞の観察では87%観察された（Table 2）．異常な4シグナルが観察された分裂期細胞をFig. 6 A及びその拡大図B, Cに示す．

Table 2　FISH analysis of three human cancer cell lines

Cell line	Judge	DNA probe			
		Chromosome 1	Chromosome 4	*c-myc*	
				metaphase	interphase
HeLa S3	normal	0%	93%	0%	3%
	aberrant	100%	7%	100%	97%
	No. of cells observed	82	100	50	100
HOS	normal	0%	0%	61%	87%
	aberrant	100%	100%	39%	13%
	No. of cells observed	139	177	135	200
OUMS-27	normal	0%	87%	7%	1%
	aberrant	100%	13%	93%	99%
	No. of cells observed	83	38	41	200

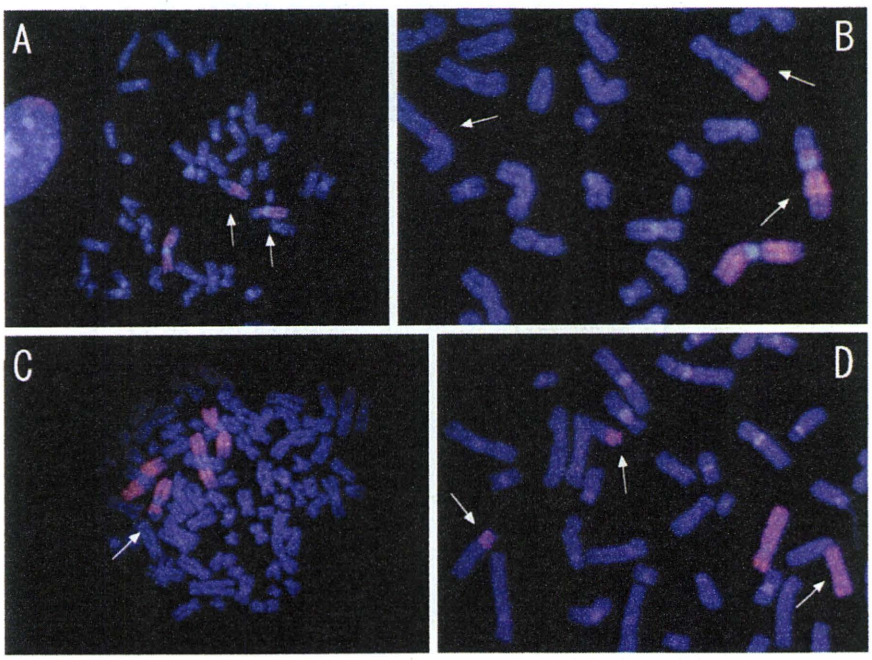

Fig. 5　FISH analysis with chromosome specific DNA probes for chromosome 1 or chromosome 4
Images are merged with whole chromosomes stained with DAPI (blue) and portions painted with SpectrumOrange (pink). White arrows indicate chromosomes with aberrations involving chromosomes 1 or 4.
A: A translocation (arrows) observed in hMSC (10796). Three chromosomes are painted in whole or in part showing a normal chromosome 1 and a translocation involving another chromosome 1.
B: A translocation and an insertion observed in an osteosarcoma derived cell line, HOS. Four chromosomes are painted in whole or in part showing a normal chromosome 1 and a translocation and an insertion involving another chromosome 1.
C: An incomplete translocation observed in a chondrosarcoma derived cell line, OUMS-27. Four chromosomes are pained in whole or in part showing three normal chromosomes 1 and an incomplete translocation involving another chromosome 1.
D: A translocation and an insertion observed in HOS. Four chromosomes are pained in whole or in part showing a normal chromosome 4 and a translocation and an insertion involving another chromosome 4.

一方，OUMS-27細胞ではほとんどの細胞が異常な*c-myc*シグナルを示した．間期細胞で観察された異常シグナルをFig. 6 Dに示す．これら一定の距離を保ったペアのシグナルは１本の染色体内での増幅の可能性が高い．HeLa細胞の分裂中期像で観察された１本の８番染色体内に*c-myc*の遺伝子座が２ヶ所ある増幅をFig. 6 Eに，それに相当する間期細胞のシグナルをFig. 6 F に示す．

*c-myc*異常頻度が異なったHOSとOUMS-27を用いて，染色体（分裂期細胞）と間期細胞での*c-myc*シグナル数の詳細な比較を行った（Fig. 7）．HOS細胞では分裂期細胞でも間期細胞でも正常２シグナルを示す細胞が圧倒的に多く，シグナル数も１から６シグナルと同じであった．OUMS-27細胞では，異常４シグナルを示す細胞が多く，シグナル数も２から８以上と似ていた．この結果から，間期細胞の観察で染色体観察の代用が可能であると考えられた．増殖が低下した時期の細胞も間期細胞で観察することにより，充分な数の細胞を解析対象とすることができより客観性の高い結果を導き出すことにつながると考えられる．

癌細胞株の染色体異常解析（Table 2）では，予想されたとおり高頻度の染色体異常が検出されたが，同じ細胞でもその異常頻度は用いるプローブによって大きく異なることが判明した．このことは，異常解析には少なくとも２種のプローブの使用が望ましいことを示唆していると考えられる．

３－３－２　hMSCでのFISH法による染色体異常解析

最も長期に継代を行えたhMSC10909を用いて，分裂が非常に低下した継代後期の細胞まで解析を行なうために，*c-myc*をプローブとして間期細胞で解析した．安全

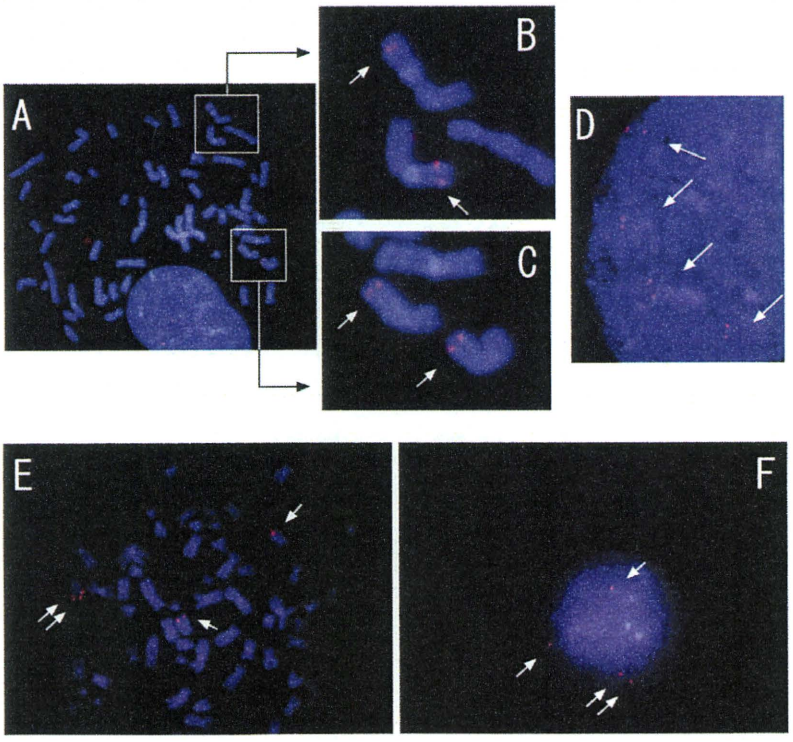

Fig. 6　FISH analysis with a locus specific identifier for *c-myc*
A: Four pairs of signals observed in a metaphase spread of an osteosarcoma derived cell line, HOS.
B: The magnified image of a part of panel A. Two pairs of signals for *c-myc* are seen near the distal end of two chromosomes. Both chromosomes seem to be translocated between chromosome 8 and chromosome 1 that has a white portion (heterochromatin) near the centromere.
C: The magnified image of another part of panel A. Two pairs of signal for *c-myc* are seen on two normal chromosomes 8.
D: Four pairs of signals for *c-myc* observed in an interphase cell of a chondrosarcoma derived cell line, OUMS-27. Panel D is a part of the interphase cell and the pair of signals seems to be amplification of *c-myc* within a chromosome, that is to say that a single signal corresponds to a pair of signals in panels B or C. Refer to panels E and F.
E: Four pairs of signals observed in a metaphase spread of HeLa cells. Two pairs of signals are seen in a chromosome located on the left. They seem to be amplification of *c-myc* within a chromosome, because only a pair of signals for *c-myc* exists in a normal chromosome 8.
F: Four signals observed in an interphase cell on the same preparation as panel E of HeLa cells. Four signals are separated in three regions. In a region, two signals are adjacent indicating that they correspond to two pairs of signals (amplification of *c-myc*) seen within a chromosome in panel E.

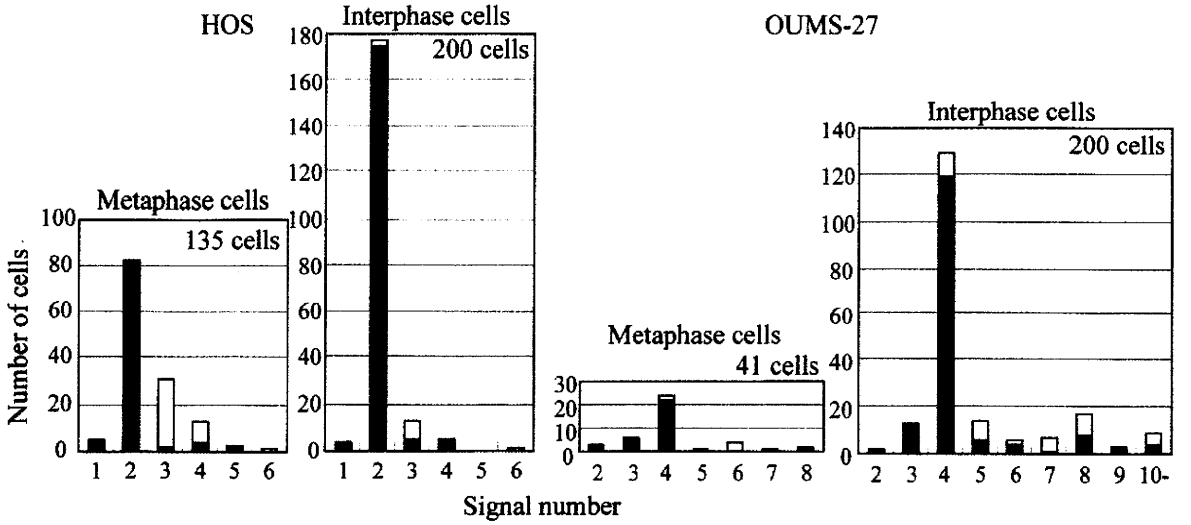

Fig. 7 Comparison of the signal number for *c-myc* observed in between metaphase cells and interphase cells in HOS and OUMS-27

The number in the upper right corner indicates the number of cells observed. The white portion of the bar indicates cells with amplification of *c-myc* within a chromosome. The black portion indicates cells without amplification within a chromosome. The distribution of the signal number observed are consistent between in the metaphase cells and in the interphase cells in both cell lines.

性評価法を標準化するために必要な，観察細胞数，統計処理法を検討するために，観察は，1枚のスライド標本上で，100細胞単位で，連続する10カ所について，計1000細胞の計数を行なった．*c-myc*は正常細胞では2シグナル観察されるため，3シグナル以上のシグナルを有する細胞を異常細胞とした．結果をFig. 8に示す．14代目では殆ど増殖しておらず標本上の細胞も少なかったために6カ所，計600細胞しか観察できなかった．その結果，1代目では10カ所の観察で異常頻度に2%から12%までのばらつきがみられた．継代3代目，5代目では，継代1代目に比べて異常頻度のばらつきは少なく，異常頻度も低かった．このことは，解凍直後の細胞はまだ培養環境に順化していないため各細胞によって増殖開始時期が一定ではなく，本来の各種細胞の構成比を反映していなかったのではないかと推察している．細胞継代10代目ではすべて6%以上の頻度を示し，観察場所によるばらつきも少なかった．継代14代目では異常頻度は明らかに増加した．

Fig. 8のデータを用いて解析に必要な観察細胞数を検討した．解析法を標準化する場合には一定の観察細胞数で1回観察した結果を用いて培養時期の異なる細胞の比較を行なうことから，検定には χ^2 検定を用いることにした．1代目と14代目の結果には必ず有意差が認められるという条件を満足する観察細胞数を探した．観察細胞数100の場合には，例えば，1代目で12%，14代目で11%の異常が観察された場合には，有意差が認められない．次に，Fig. 8のデータを最初から200個ずつ計数した

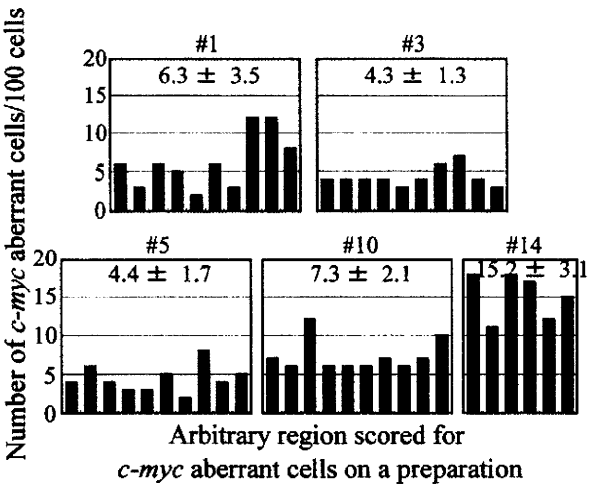

Fig. 8 Distribution of the number of *c-myc* aberrant cells observed on 100 cells during five months passage in hMSC (10909)

The number of *c-myc* aberrant cells per 100 cells was scored at 10 regions on a chromosome preparation, except for #14 where the number was scored at six regions due to less number of cells. The number in the top of graphs indicates the average number of *c-myc* aberrant cells ±SD in ten or six regions analyzed.

として，5ケ所の計数結果と14代目についても同様に3ケ所の計数結果の間のすべての組み合わせで χ^2 検定を行なった．この時も有意差が認められない場合があった．同様に300細胞と細胞数を増やして検討した結果，300細胞以上で1代目と14代目の間には必ず有意差がつくことが判明した．

そこで，他の２ロットのhMSCについても300細胞を観察し，χ^2 検定を行なった．その結果をTable 3に示す．Lot. 10796では５代目までしか解析できなかったが，*c-myc*異常細胞の有意な増加は認められなかった．Lot. 11809では１ヵ月で有意差のある異常細胞の増加が認められた．Lot. 10909はFig. 8のデータを表にしたものであるが，14代目で有意差のある異常細胞の増加が認められた．本研究で用いたhMSCは１社から購入しており細胞の調製は同じ製造管理工程のもとで同様に実施されていると考えられることから，この表でのロット差はドナー差，つまり臨床での個人差に相当すると考えられるが，３ロットの間でも差が認められる．例えば，ロット11809の１代目での異常細胞数を基準にすると，ロット10796は１代目からすでに有意差のある異常細胞数を示していることになる．*In vitro*継代培養による異常頻度の変化の有無を判定するには，患者本人の採取直後の細胞の異常を慎重に観察する必要があると考えられる．

遺伝子座プローブだけでなく染色体特異的DNAプローブを用いる構造異常の解析も安全性評価指標の候補としていたが，Table 3に示すように，分裂指数から判断してロットによっては培養初期の標本でさえ充分な数の分裂期細胞を集めることが困難であることが判明した．しかしながら，基礎データとして染色体構造異常の頻度に関するデータも確認しておく必要があると考え，hMSC 10796の１代目の標本で１番と４番染色体プローブ，比較的増殖が良かったhMSC 10909で１番染色体での５代目までの解析を試みた（Table 4）．また，別ロットhMSCの５代目での解析を参考に記載する．１番染色体プローブを用いた解析ではhMSC 10796は1.6%の細胞が転座（Fig. 5 A）を示し，別ロットのhMSCは継代５代目で２%の細胞が転座を有していた．４番染色体では１代目でも別ロットの５代目でも異常は検出されなかった．hMSC 10909では１，３，５代目の細胞を200個以上観察したが，継代による異常頻度の増加は認められなかった．

Table 3 Number of c-myc aberrant cells in interphase cells of hMSC

hMSC Lot.	Passage	Days in culture	Mitotic index(%)	No. of aberrant cells / 300 cells	χ^2-test
10796	#1	0	2.8	24	—
	#3	13	NT	35	N.S.
	#5	31 (1 month)	0.2	23	N.S.
10909	#1	0	10.2	15	—
	#3	13 (2 weeks)	5.6	12	N.S.
	#5	27 (4 weeks)	7.2	14	N.S.
	#10	78 (2.5 month)	0.1	25	N.S.
	#14	152 (5 month)	0.6	47	$P<0.001$
11809	#1	0	1.5	10	—
	#5	28 (1 month)	0.8	23	$P<0.05$
	#8	66 (2 month)	NT	41	$P<0.001$
	#10	98 (3 month)	NT	44	$P<0.001$

NT; Not tested, N.S.; Not significant.

Table 4 FISH analysis with chromosome specific DNA probes for chromosomes 1 and 4 in hMSC

Passage	Judge	hMSC 10796 Chromosome 1	hMSC 10796 Chromosome 4	hMSC 10909 Chromosome 1
#1	normal	98.4%	100%	95.8%
	aberrant	1.6%	0%	4.2%
	No. of cells observed	60	207	261
#3	normal			97.9%
	aberrant			2.1%
	No. of cells observed	NT*	NT	242
#5	normal	98.0%	100%	96.2%
	aberrant	2.0%	0%	3.8%
	No. of cells observed	201**	55**	236

*NT: Not tested. **The data are derived from another lot of hMSC.

4．考察

hMSCの無限増殖能を制御できなくなった場合として癌化を危惧したが，本研究での３ロットのhMSCについては，継代による増殖低下，細胞形態の変化，老化細胞染色から，「生体から分離し，*in vitro*の培養系に移したhMSCは無限増殖能を示さない」ことが判明した．むしろ，hMSCは*in vitro*で長期継代培養することによって老化徴候を示すようになると考えられた．また，老化染色写真Fig. 2に示すように，継代13代目で殆ど増殖をしなくなっているにも拘わらず，すべての細胞が老化（関連）細胞ではなかった．以上のことはhMSCの他のロットについても確認している[3]．幹細胞の増殖分化を考える時，従来は一つの幹細胞が単純に増殖を繰り返して細胞数を増やす時期があり，その後その細胞集団が何らかの分化刺激を受けて全体が分化していくという流れが考えられていた．近年，幹細胞が分裂する時娘細胞の一つは自己複製のための幹細胞であるが，他の一つはすでに分化（の準備ができた）細胞になっており，後者はその後分裂せず前者が同じ形式の分裂を繰り返すことにより分化（の準備ができた）細胞が増え，それらと一定数の無限増殖能をもった幹細胞とからなる細胞集団が考えられてきている．従来の考え方ではある時期の細胞集団は同じ性質をもった細胞の集まりであるが，後者の考え方ではヘテロな細胞集団となる．本研究の老化関連染色において継代を重ねた細胞でもすべての細胞が青く染まらなかったことは，後者の考え方を導入すると理解しやすいと考えられる．

Table 4に示すように，充分な数（例：200細胞）の分裂中期像があっても４番染色体は誘発される異常頻度が低く，解析細胞数を多くする必要が考えられることから，本目的の解析には適切ではないと考えられる．２例

の健常人の末梢血リンパ球で同じ手法で4番染色体プローブでの解析を行なった経験があるが，異常頻度は0.13%あるいは0.11%であり，現実的には約800細胞を観察してやっと1個の異常細胞を検出できる程度であった[4]．また，癌細胞でさえも4番染色体の異常頻度は極端に低いものがあった（Table 2）．

一方，1番染色体ではTable 4に示すように，60細胞の観察ですでに1個の異常を検出できており，4番染色体より異常頻度が高いことが予想され，100細胞程度の観察でも異常頻度を算出でき，*in vitro*培養前後の比較が可能だと考えられる．1番染色体の方が解析プローブとして適切であると考えられるが，基本的にhMSCの標本では安定した数の分裂中期像を集めることが困難という事実から，染色体を観察対象とする評価は困難だと考えられた．

対照的に，*c-myc*では間期細胞での効率のよい異常解析が可能で，安全性評価法として有用であることが示唆された．実際に，5ヵ月まで継代培養できたhMSC 10909を用い間期細胞で*c-myc*解析を行なった結果，継代による異常頻度の変化，及び最終継代標本で有意な増加を検出できた（Table 3）．

本研究では実施していないが，分化により増殖が停止した細胞でも本研究と同様に細胞標本を作製し，間期細胞でFISHによる観察が可能であると考えられる．ただし，骨芽細胞のように分化によって骨化する細胞ではカルシウム沈着がおこり細胞標本を作製できない可能性がある．このような細胞では遺伝的影響の検出は困難であると考えられる．

試験手技上の利点であるが，解析対象を間期細胞にすることによって，標本作製も容易になり観察時間も短縮できる．広く一般に応用するにあたっては非常に重要な長所である．具体的には，この手法を用いれば最短3日（標本作製1日，翌日FISH，3日目に300細胞を観察）で結果を得ることができ，臨床手順の流れをさえぎることなくこの結果を臨床に反映させることができると考えられる．

hMSCは市販品であるが，Cambrex社によるとドナーから細胞を採取後製品とするまでに約3週間（2－3代の継代）を要しているという．従って，1ヶ月で統計学的に有意な異常頻度を示したhMSC11809（Table 3）はその時点でヒトから採取後すでに2ヵ月近く培養していることになる．現在臨床研究で行なわれている培養は採取後長くて1ヵ月といわれており，Table 3の結果から，実際的にはその期間では異常細胞頻度が有意に増加することはないであろうと考えている．5ヵ月まで継代した時点で*c-myc*の明らかな異常の増加が認められたhMSC 10909でも，1ヵ月までは染色体数の分布も46本にピークが認められ（Fig. 3），*c-myc*の異常頻度も培養開始直後の頻度より高くはなかった．

*c-myc*等の遺伝子座での異常とは別に染色体の構造異常も指標とするのが望ましいと考えられるが，効率よく異常を検出できることが判明したFISH法でも，分裂期細胞での観察は実際的には困難であることが判明した．染色体構造異常を間期細胞で観察する方法として小核試験があり検討の余地ありと考えられるが，今後の課題としたい．

最後に，「*In vitro*培養ヒト間葉系幹細胞の安全性評価法」の1つとして，以下の方法を提案したい．

1）提案の前提：採取された幹細胞の本来使用目的以外の使用量を最小限にする．臨床手順を妨げない．

2）観察対象：患者から採取直後の細胞（陰性対照）と，*in vitro*で培養増殖させ患者に移植直前の細胞とで，異常頻度の比較を行う．

3）評価手法：3－1．位相差顕微鏡による細胞形態観察

3－2．FISH法で300間期細胞の染色体異常解析を行い，χ^2 検定を行う．プローブは*c-myc*等の遺伝子座特異的DNAプローブ2種を用いる．

謝辞

本研究は財団法人ヒューマンサイエンス振興財団よりの研究助成金によって実施された．ここに謝意を表する．

参考文献

1）Dimri, G. P., Lee, X., Basile, G., Acosta, M., Scott, G., Roskelly, C., Medranos, E. E., Linskens, M., Rubelj, I., Pereira-Smith, O., Peacocke, M. and Campisi, J.: *Proc. Natl. Acad. Sci. USA*, **92**, 9363-9367 (1995)

2）Matsuoka, A., Tucker, J. D., Hayashi, M., Yamazaki, N. and Sofuni, T.: *Mutagenesis*, **9**, 151-155 (1994)

3）Ito, T., Sawada, R., Fujiwara, Y., Seyama, Y. and Tsuchiya, T.: Biochem. Biophys. Res. Commun., **359**, 108-114 (2007)

4）Matsuoka, A., Yamada, K., Hayashi, M. and Sofuni, T.: *J. Radiat. Res.*, **37**, 257-265 (1996)

Effects of surface chemistry prepared by self-assembled monolayers on osteoblast behavior

Ryusuke Nakaoka,[1] Yoko Yamakoshi,[2] Kazuo Isama,[1] Toshie Tsuchiya[1]

[1]Division of Medical Devices, National Institute of Health Sciences, 1-18-1 Kamiyoga, Setagaya-ku, Tokyo 158-8501, Japan
[2]Departments of Radiology and Department of Chemistry, University of Pennsylvania, 231 S. 34th Street, Philadelphia, Pennsylvania 19104-6323

Received 27 August 2008; revised 8 October 2009; accepted 1 November 2009
Published online 22 February 2010 in Wiley InterScience (www.interscience.wiley.com). DOI: 10.1002/jbm.a.32714

Abstract: A surface of biomaterials is known to affect the behavior of cells after their adhesion on the surface, indicating that surface characteristics of biomaterials play an important role in cell adhesion, proliferation, and differentiation. To assess the effects of functional groups on biomaterial surface, normal human osteoblasts (NHOsts) were cultured on surfaces coated with self-assembled monolayers (SAMs) containing various functional groups, and the adhesion, proliferation, differentiation, and gap junctional intercellular communication (GJIC) of the NHOsts were investigated. In the case of SAM with terminal methyl groups (hydrophobic surface), NHOst adhesion and proliferation was less prevalent. In contrast, NHOsts were adhered well on SAMs with hydroxyl, carboxyl, amino, phosphate, and sulfate group, which are relatively hydrophilic, their proliferation and differentiation level were dependent on the type of functional groups. Especially, when they were cultured on either SAMs with phosphate or sulfate group, both their alkaline phosphate activity and the calcium deposition by them were enhanced more than those cultured on a collagen-coated dish. More interestingly, GJIC of NHOsts, which has been reported to play a role in cell differentiation as well as homeostasis of cells, were not significantly different among the SAM surfaces tested. These suggest that a specific functional group on a material surface can regulate NHOst adhesion, proliferation, and differentiation *via* cell-functional group interaction without influencing their homeostasis. © 2010 Wiley Periodicals, Inc. J Biomed Mater Res Part A: 94A: 524–532, 2010

Key Words: self assembled monolayer, surface chemistry, cell differentiation, gap junctional intercellular communication

INTRODUCTION

Many cellular responses followed by an interaction with the biomaterials are mediated through signal transductions triggered by cellular recognition of their surface characteristics. Cells first recognize proteins adsorbed on the biomaterials, followed by various cellular responses. The extracellular matrix (ECM), consisting of numerous kinds of molecules such as proteins, polysaccharides, and proteoglycans, regulates the behavior of surrounding cells via the integrins to form tissues and organs precisely.[1,2] As the ECM provides an essential three-dimensional environment for cells to construct the tissues, many researches focused on the improvement of biocompatible materials by their modification, including artificial ECMs. It is known that first proteins, such as fibronectin and vitronectin, adsorb firstly onto the surface of materials, followed by cell adhesion onto the surface via recognition of the proteins. The modification of biomaterial surfaces with various peptides or proteins composing the ECM can result in the improvement of the adhesion, proliferation, and differentiation of the cells.[3–8] It has been reported that conformation and adhesion behavior of proteins are influenced by the surface characteristics of the materials, and functions of cells adhering on the surface are regulated via the structure of the adsorbed proteins,[9] indicating that surface characteristics of the materials are important factors in controlling cell behavior in desired manner via adsorbed proteins. Thus, a systematic control of surface characteristics may be one way to regulate cell behavior interacted with the surface, in other words, it can regulate the biocompatibility of biomaterials.

During this decade, many studies on self-assembled monolayers (SAMs) of alkanethiolates on gold to control interfacial characteristics have been reported.[10–14] Long-chain alkanethiolates can adsorb onto a gold surface in the solution forming well-packed and highly oriented monolayers by the specific reaction of thiol to gold and van der Waals interaction of long alkyl chain. By using alkanethiolate derivatives with terminal functional groups, a surface modified with a specified functional group can be prepared easily to study an interaction between the simplified model material surface covered with the specified functional group and cells. Many studies of cell behavior on SAM surfaces with systematic patterns from hydrophobic and hydrophilic groups have been reported, but studies on an effect of specific functional groups such as amino (positively charged group), phosphate (possible site to initiate hydroxyapatite

Correspondence to: R. Nakaoka; e-mail: nakaoka@nihs.go.jp
Contract grant sponsors: Health and Labour Sciences Research Grants for Research on Advanced Medical Technology; Research on Regenerative Medicine and Research on Regulatory Science of Pharmaceuticals and Medical Devices by Ministry of Health, Labour and Welfare

nucleation), and sulfate groups are not easily found although these groups can be expected to affect cell behavior via interaction with endogenous growth factors. We have been working on this and have reported that polysaccharides modified with sulfated groups enhance differentiation level of interacted cells *in vitro*,[15] suggesting a preferable property of sulfated groups on biocompatibility of materials. Therefore, studies on an interaction between a specified functional group such as a sulfated group and cells will satisfy one of our interests in mechanisms of sulfated groups on cell fate, and give valuable information of key factors regulating biocompatibility of various biomaterials.

In this study, various SAM surfaces covered with a specific functional group, such as alkyl, carboxyl, hydroxyl, amino, phosphorylated, or sulfated group, were prepared. After culturing normal human osteoblasts (NHOsts) on each surface, their proliferation and differentiation levels were measured to evaluate influences of surface functional groups on cell behavior. Also gap junctional intercellular communication (GJIC) level of the NHOsts on various SAM surfaces was measured, as this has been reported to play a very important role in the maintenance of cell homeostasis,[16] and we have been interested in the effects of model biomaterials on the GJIC level of the cells as an index of biocompatibility of biomaterials.[17–22] In this study, basic findings of interaction between cells and surface functional groups are described, which will be important for designing more biocompatible and functional biomaterials in the near future.

MATERIALS AND METHODS

Chemicals

Chemicals for the preparation of SAM surfaces such as 11-hydroxy-1-undecanethiol, 10-carboxy-1-decanethiol, and 11-amino-1-undecanethiol, were purchased from Dojindo laboratories (Kumamoto, Japan). The 1-dodecanthiol and other chemicals used for the preparation of SAM-OSO_3H and SAM-OPO_3H_2 were purchased from Wako Pure Chemicals, Inc. (Osaka, Japan) unless stated.

Preparation of gold-coated coverslips

Gold-coated coverslips for the experiments were prepared by ion spattering coating of gold with 15 nm in thickness onto glass coverslips (Matsunami Glass Ind., Ltd. Osaka, Japan) using JFC-1500 (JEOL Ltd., Tokyo, Japan). For the preparation of SAM with terminal methyl groups (SAM-CH_3), coverslips were precoated with chromium (1 nm in thickness) by electron-beam evaporation to avoid detaching the gold coating due to the hydrophobicity of the SAM surface.

Preparation of self-assembled monolayer (SAM)-covered coverslips (SAM-CH_3, SAM-OH, SAM-COOH and SAM-NH_2)

A SAM surface covered with terminal methyl (SAM-CH_3), hydroxyl (SAM-OH), carboxyl (SAM-COOH), or amino group (SAM-NH_2) on a coverslip was prepared by simply immersing a gold-coated coverslip into ethanol solution (1 m*M*) of

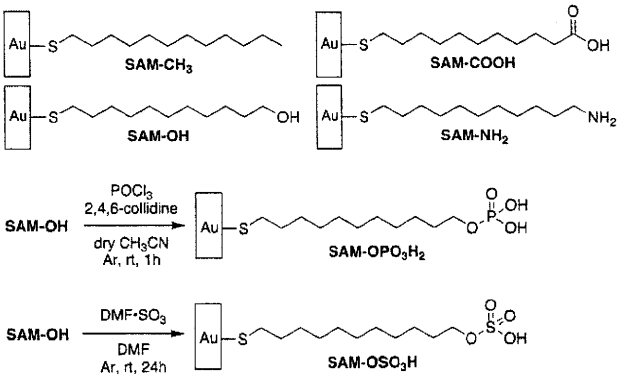

FIGURE 1. A schematic description of SAM surfaces prepared in this study.

corresponding commercially available alkanethiol derivatives for 24 h at room temperature. The obtained SAM-covered coverslips were washed by ethanol for several times, followed by drying *in vacuo*. The obtained SAMs are schematically described in Figure 1.

Preparation of SAM-OPO_3H_2-covered coverslip

A phosphorylated SAM surface (SAM-OPO_3H_2) was prepared using the method described by Tanahashi and Matsuda.[23] Briefly, the gold-coated coverslip covered with SAM-OH was phosphorylated by the addition of 0.2*M* phosphorus oxychloride and 0.2*M* 2,4,6-collidine in dry CH_3CN under Ar atmosphere. The reaction was carried out for 1 h at room temperature under Ar atmosphere. The resulted coverslip with SAM-OPO_3H_2 was then washed with CH_3CN thoroughly, and water for several times, then dried *in vacuo* at room temperature. Scheme of this reaction is shown in Figure 1.

Preparation of SAM-OSO_3H-covered coverslip

A sulfated SAM surface (SAM-OSO_3H) was prepared by sulfation of hydroxyl groups using sulfertrioxide dimethylformamide complex (DMF-SO_3), which was originally reported as a sulfation method of hydroxyl groups of polysaccharides.[21,24] Briefly, the coverslip of SAM-OH was immersed in dry *N,N'*-dimethylformamide (DMF), followed by the addition of DMF-SO_3 (Sigma-Aldrich, St. Louis, MO) under Ar atmosphere. The reaction was carried out for 24 h at room temperature under Ar atmosphere. The obtained coverslip with SAM-OSO_3H was washed for several times with DMF and water, and then dried *in vacuo* at room temperature. A scheme of this reaction is shown in Figure 1 as well.

Surface characterization of SAM-covered coverslips

Water contact angles of all prepared SAM-covered coverslips were measured with the sessile drop method. More than five measurements were carried out for each SAM-covered coverslip. Surface chemical compositions of the SAM-covered coverslips were analyzed by electron spectroscopy for chemical analysis (ESCA-3200, Shimadzu Co., Kyoto, JAPAN).

Cell culture

Normal human osteoblasts (NHOst) were purchased from Lonza Walkersville Inc. (Walkersville, MD, USA). The standard culture of NHOst was performed using alpha minimum essential medium (Gibco, Grand Island, NY) containing 20% fetal calf serum (FCS) (Kokusai Shiyaku Co., Ltd., Tokyo Japan). The cells were maintained in incubators under standard conditions (37°C, 5 %-CO_2-95 %-air, saturated humidity). All assays were performed using alpha minimum essential medium containing 20% FCS, supplemented with 10 m*M* beta-glycerophosphate. The various SAM-covered coverslips were placed in the wells of 12-well plates and NHOsts (4×10^4 cells/well/1 mL medium) were inoculated on them. In each experiment, the medium was changed for three times and their differentiation level was evaluated after a 1-week incubation.

Proliferation and differentiation of NHOsts cultured on various SAM-covered coverslips

The proliferation of NHOst cells cultured on SAM-covered coverslips was estimated by Tetracolor One assay reagent (Seikagaku Co., Tokyo, Japan), which incorporates an oxidation–reduction indicator for detecting cellular metabolic activity. After a 1-week incubation of NHOsts, 50 μL of Tetracolor One solution was added to each test dish filled with 1 mL of a culture medium, followed by a further 2 h incubation. The absorbance of the supernatant at 450 nm was measured by μQuant spectrophotometer (Bio-tek Instruments, Inc., Winooski, VT).

Estimation of alkaline phosphatase (ALP) activity was performed according to an original procedure by Ohyama et al.[25] After estimating the proliferation of the NHOst cells cultured on the SAM-covered coverslips, the cells were washed by phosphate-buffered saline (PBS(−)), followed by the addition of 1 mL of 0.1*M* glycine buffer (pH 10.5) containing 10 m*M* $MgCl_2$, 0.1 m*M* $ZnCl_2$, and 8 m*M* *p*-nitrophenylphosphate sodium salt. After incubating the cells at room temperature for 7 min, the absorbance of the solution at 405 nm was detected using μQuant to evaluate the ALP activity of the tested cells.

The amounts of calcium deposited by the cell during a 1-week incubation were measured as follows. After fixing the cells in PBS(−) containing 3% formaldehyde, the cells were washed with PBS(−), and then 0.5 mL of 0.1*M* HCl was added to each well. The amounts of calcium dissolved in HCl were estimated using a calcium detecting kit (Calcium-C test Wako, Wako, Osaka, Japan) according to manufacturer's instruction.

Measurements of GJIC activity

NHOst cultured on SAM-covered coverslips were subjected to fluorescence recovery after photobleaching (FRAP) analysis to evaluate the effect of these surfaces on the GJIC. FRAP analysis was carried out according to the procedure of Wade et al.[26] with some modifications.[20] Briefly, NHOst were plated and incubated for 1 day on the SAM-covered coverslips. After incubated with a fluorescent dye, 5,6-carboxyfluorescein diacetate in PBS(−) containing calcium and magnesium, the cells contacting at least two other cells were subjected to FRAP analysis under Ultima-Z confocal microscope (Meridian Instruments, Okemos, MI). The cells were photobleached with a 488 nm beam, and recovery of fluorescence intensity was subsequently monitored for 4 min. The data obtained from more than seven independent cells were expressed as the average ratio of the fluorescence recovery rate to the rate obtained from NHOst cultured on a collagen-coated dish as standard experiments.

Connexin 43 mRNA expression in NHOsts

To estimate effects of the surface functional group on mRNA expression of connexin 43 protein, which plays an important role in GJIC by forming channels between neighboring cells, a real time PCR technique was applied. Briefly, total RNA from NHOsts cultured on various functional groups was isolated by RNeasy microprep kit (QIAGEN, Valencia, CA) per the manufacturer's instruction. After its reverse transcription, a real time PCR was performed utilizing the primers for connexin 43, LightCycler FastStart DNA master SYBR green I kit (Roch Applied Science, Penzberg, Germany) and LightCycler 4 (Roche Applied Science). To normalize the data, mRNA expression of a housekeeping gene, glyceraldehyde 3-phosphate dehydrogenase (GAPDH), was also determined using LightCycler primer set for GAPDH (Roche Applied Science). Primer sequences for connexin 43 are shown below:

Forward: 5′-GGGCTAATTACAGTGCAG-3′
Reverse: 5′-CATGTCCAGCAGCTAGTT-3′

Statistic analysis

All data were expressed as mean values ± standard deviation of the obtained data. The Fisher-Tukey criterion, calculated by inerSTAT-a v1.3 (freeware, published by Instituto Nacional de Enfermedades Respiratorias), was used to control for multiple comparisons and to compute the least significant difference between means.

RESULTS

Table I shows contact angle against water and elemental signal ratios of prepared coverslips covered with various SAMs. The signal ratio against a carbon signal detected in the same surface by ESCA was calculated from the signal area and the sensitivity factor of each element. If a signal area recorded on ESCA was lower than 10^3 or the calculated value was lower than 1×10^{-3}, the results were not described in the table. As shown in Table I, contact angle measurements revealed that while SAM-CH_3 had a hydrophobic surface, others SAMs except for SAM-NH_2 had hydrophilic ones compared with the intact gold-coated surface. The contact angle of SAM-OH was significantly lower than any other SAM surfaces. After a reaction from SAM-OH to SAM-OPO_3H_2, the contact angle was significantly increased, suggesting that the reaction proceeded successfully. Also as shown in Table I, the ratios of atomic concentration of nitrogen, phosphorus, and sulfur (N/C, P/C, and S/C) calculated from raw signal areas were detected only from SAM-NH_2, SAM-OPO_3H_2, and SAM-OSO_3H, respectively, indicating that

TABLE I. Surface Characterization of SAMs by Contact Angle and Elemental Signal Ratios Against Carbon

		SAMs Modifying Surfaces					
	Gold (Control)	SAM-OH	SAM-OSO_3H	SAM-COOH	SAM-OPO_3H_2	SAM- NH_2	SAM-CH_3
Contact Angle	64.4 ± 2.1	40.1 ± 14.2*,†	44.3 ± 10.2	51.7 ± 14.5	59.0 ± 13.7*	65.0 ± 9.8	102.9 ± 3.0†
Elemental signal ratios							
O/C	3.2×10^{-3}	2.9×10^{-3}	6.8×10^{-3}	4.6×10^{-3}	4.8×10^{-3}	2.2×10^{-3}	–
N/C	–	–	–	–	–	1.8×10^{-3}	–
P/C	–	–	–	–	2.1×10^{-3}	–	–
S/C	–	–	2.2×10^{-3}	–	–	–	–

* $p < 0.05$ between SAM-OH and SAM-OPO_3H_2.
† $p < 0.01$ against Au.

all desired SAM surfaces with specific functional groups were successfully prepared.

Figures 2 and 3 show light micrographs of NHOsts cultured on each SAM surface for 1 day and 1 week. When NHOsts were cultured on a gold-coated coverslip for 1 day, the number of NHOsts observed was apparently lower [Fig. 2(B)] than that on a collagen-coated culture plate [Fig. 2(A)]. After 1-week incubation, the surface of gold-coated coverslip was fully covered with NHOsts, indicating that the NHOsts could proliferate on the intact gold surface [Fig. 3(B)]. The numbers of NHOsts adhered on the gold surface with various SAMs were influenced by the functional groups covering the SAMs as follows. Less NHOsts could adhere on a SAM-CH_3, the most hydrophobic surface among the SAM surfaces used in this study, than those on the gold surface [Figs. 2(C) and 3(C)]. The NHOsts on the SAM-CH_3 were tended to aggregate after 1-day culture [Fig. 2(C)] and likely to detach from the surface during 1-week culture as no aggregates and few stretched NHOsts were observed after 1 week [Fig. 3(C)]. On the other hand, NHOsts adhered on other SAM surfaces such as SAM-COOH, SAM-OH, SAM-OPO_3H_2 and SAM-OSO_3H could be observed more than on the gold surface, as shown in Figure 1(D,E,G,H). Judging from the number of nodules observed in Figure 3, it is likely that there is no effect of functional groups in between the hydrophilic SAM surfaces on differentiation level of NHOsts.

Table II summarizes the relative amount of cell number, ALP activity, and the deposited calcium of NHOsts after 1-week culture on various SAMs. Although differentiation levels of NHOsts on hydrophilic functional groups of SAM were not significantly different by the observation of the nodule number (Fig. 3), the functional groups apparently influenced both ALP activity of the NHOsts and the amount of deposited calcium as well as the cell number ratio adhering on the surface as shown in Table II. When NHOsts were cultured on SAM-CH_3 surface, not only the cell number but also their ALP activity were low and the amount of deposited calcium per cell were under detection limit. On the contrary, when NHOsts were cultured on SAM-OH, SAM-COOH, or SAM-NH_2, the cell number, the ALP activity and the deposited calcium amounts per cell were not significantly different from those observed on a gold surface. Interestingly, when NHOsts were cultured on SAM-OPO_3H_2 or SAM-OSO_3H, their ALP activity and the amounts of calcium deposition per cell increased although the cell number ratio was about one-third to half of that observed on a gold surface.

To estimate the effects of functional groups on another cell function, GJIC level of NHOsts on various SAM surfaces were measured after 1-day incubation (Table III). In addition, expression levels of connexin 43 mRNA in NHOsts on the various functional groups were measured by real-time PCR (Fig. 4). Although it was observed that their differentiation level was influenced by the functional group on SAM surfaces, statistical differences in neither the GJIC level nor the expression level of connexin 43 mRNA during 1-week culture were observed among the SAM surfaces tested in comparison with that of NHOsts on a collagen-coated dish at the same time period of their culture.

DISCUSSION

Several studies have been reported that surface chemical properties are responsible for behavior of attached cells, for example, their adhesion, proliferation, and differentiation on the surface as well as surface topography such as microfabricated grooves and pits.[9–12,27,28] Usually, a cell adheres not directly on a surface of a material but on preadsorbed proteins on the material, originally contained in the culture medium. Interaction of the preadsorbed proteins with a material surface is important in cell attachment and protein adsorption is influenced by surface properties, such as chemical composition, surface charge, and a hydrophilicity/hydrophobicity balance of surface.[9] Therefore, SAM is an ideal surface to investigate effects of the chemical and physico-chemical property on cell behavior as the surface covered by single chemical group can be prepared easily.

Changes in contact angles and elemental signal ratio against carbon signals of the prepared SAM surfaces (Table I) indicated that SAM surfaces covered with various chemical groups could be prepared successfully by the methods described in "Materials and Methods" section. Although chlorosulfonic acid is a common reagent to convert hydroxyl groups of SAM-OH to sulfate group,[29] we used DMF-SO_3 for the preparation of SAM-OSO_3H in this study. In the trial of substitution reaction by chlorosulfonic acid, it was found to be difficult to remove all by-products adsorbed on the coverslip without detaching a gold coating, thus modest

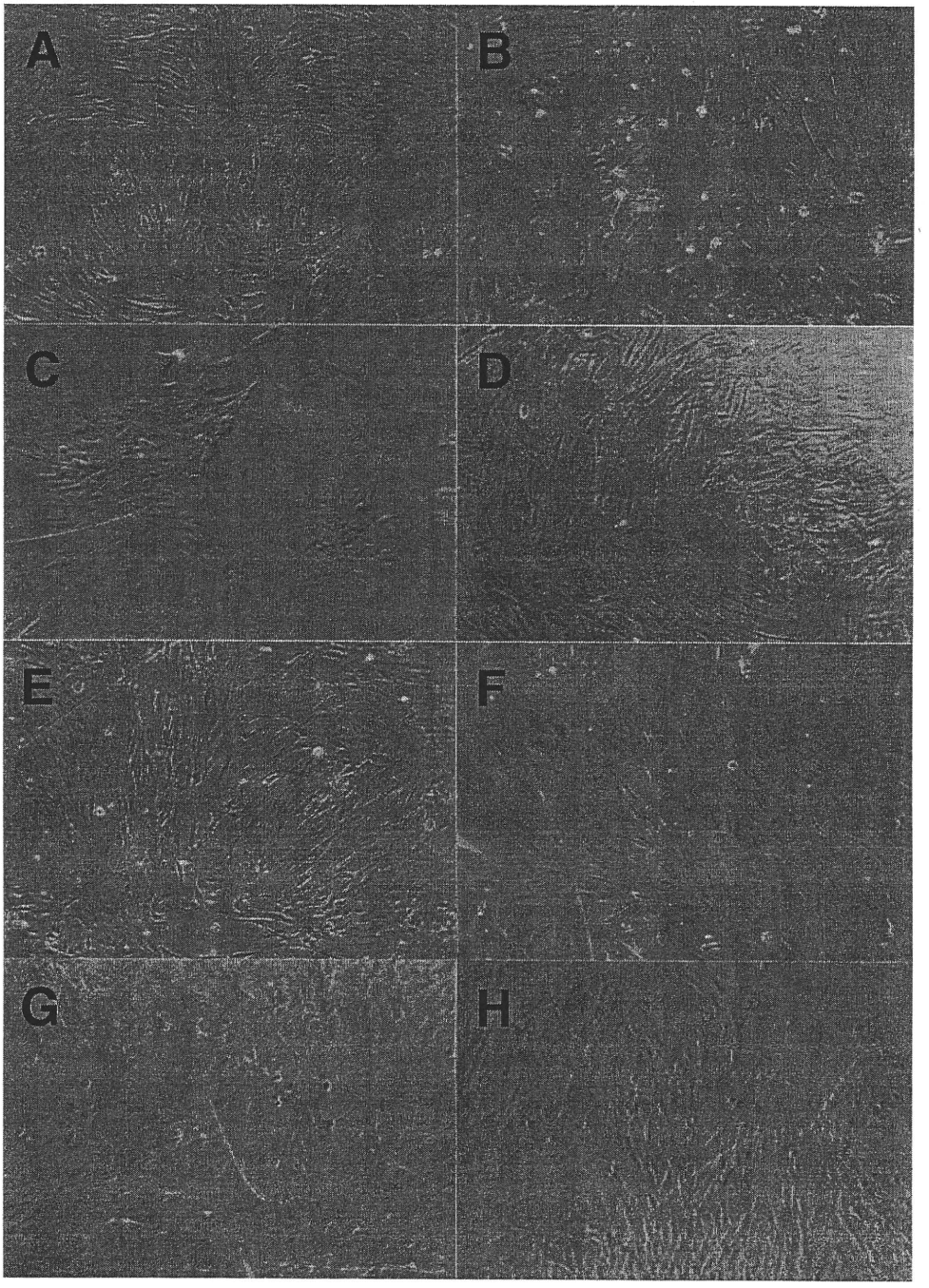

FIGURE 2. Light micrograph of NHOsts cultured on various SAM surfaces for 1 day. (Original magnification is ×40.) NHOsts were cultured on a collagen-coated dish (A), gold-coated coverslip (B), SAM-CH_3 (C), SAM-COOH (D), SAM-OH (E), SAM-NH_2 (F), SAM-OPO_3H_2 (G), and SAM-OSO_3H (H). [Color figure can be viewed in the online issue, which is available at www.interscience.wiley.com.]

condition reaction, which is often applied for sulfation reaction of hydroxyl groups in polysaccharides with fewer by-products, was employed. In fact, an apparent S/C signal was detected as shown in Table I, indicating the sulfate group was successfully introduced to the surfaces by the employed reaction in good yield.

Effect of chemical groups on cell attachment has been studied as well as protein adsorption utilizing SAM. It has been reported that the number of cell adhering on various surfaces is influenced by the physico-chemical properties of the surfaces such as hydrophilic/hydrophobic balance, which is closely related to contact angles.[11,12,27,30–33] In this study, modification of the gold surface with SAM changed the number of NHOsts adhering on the surface depending on the functional groups of the SAM (Fig. 2). Less NHOsts could adhere on a SAM-CH_3, the most hydrophobic surface among the prepared SAM surfaces, than those on the gold surface. The NHOsts observed on it were tend to aggregate

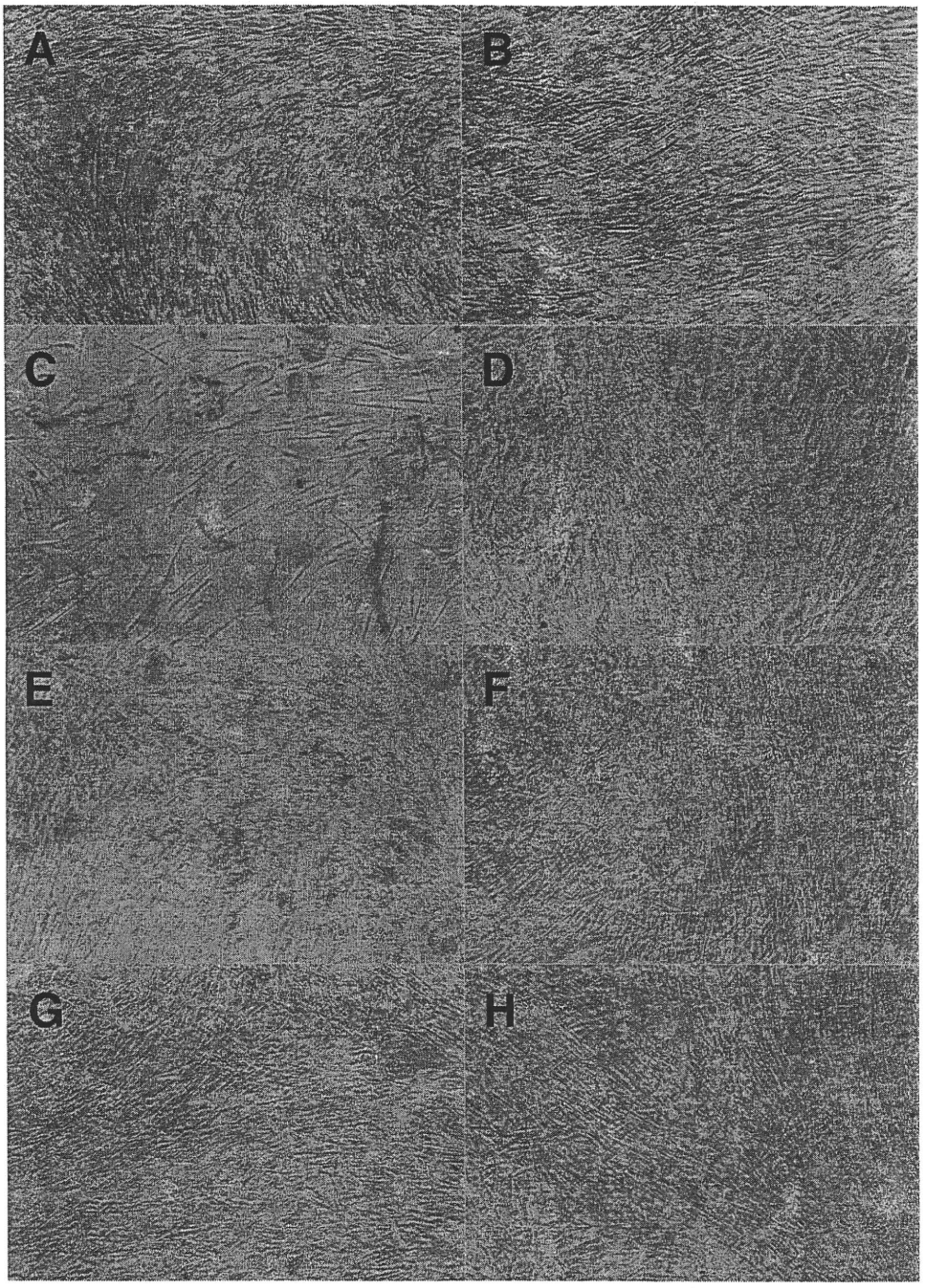

FIGURE 3. Light micrograph of NHOsts cultured on various SAM surfaces for 7 days. (Original magnification is ×40.) NHOsts were cultured on a collagen-coated dish (A), gold-coated coverslip (B), SAM-CH_3 (C), SAM-COOH (D), SAM-OH (E), SAM-NH_2 (F), SAM-OPO_3H_2 (G), and SAM-OSO_3H (H). [Color figure can be viewed in the online issue, which is available at www.interscience.wiley.com.]

and likely to detach from it during 1-week culture as no aggregates and a few stretched NHOsts were observed on it as shown in Figure 3. On the other hand, NHOsts could adhere on other SAM surfaces more than on the gold surface, indicating that the surfaces covered with functional groups such as amino, carboxyl, hydroxyl, phosphate, and sulfate groups have a suitable hydrophilic/hydrophobic balance not to interfere cell adhesion them. As adhesion and spreading behaviors of osteoblasts on materials have been reported to depend on vitronectin and fibronectin primarily adsorbed on the surfaces,[34,35] it may be indispensable to investigate an interaction between various functional groups and these two proteins influencing there adsorption behavior and possible conformation changes to clarify the mechanism of cell adhesion on the interacted-functional groups more precisely.

The ALP activity and deposited calcium amount were measured for estimating differentiation level of NHOsts

TABLE II. The Cell Number, Alkaline Phosphatase Activities, and Deposited Calcium Amounts of NHOsts Cultured on Several Kinds of Prepared SAM Surfaces after 1-week Incubation

Samples	The Cell Number Ratio (%)	$\frac{\text{ALP Activity}}{\text{The Cell Number}}$ (%)	$\frac{\text{Calcium Amounts}}{\text{The Cell Number}}$ (μg/ratio)
Gold	100.0 ± 4.9	100.0 ± 10.0	8.1 ± 1.6
SAM-OH	107.8 ± 2.2	119.7 ± 6.4	8.7 ± 2.3
SAM-OSO_3H	50.8 ± 15.4*	150.1 ± 55.0	33.4 ± 13.5
SAM-COOH	93.2 ± 33.9	100.2 ± 6.8	11.6 ± 2.5
SAM-OPO_3H_2	37.5 ± 4.2*	147.5 ± 9.4	57.0 ± 25.2**
SAM-NH_2	106.1 ± 8.6	112.1 ± 4.3	8.5 ± 1.1
SAM-CH_3	17.1 ± 10.3*	34.8 ± 26.0*	Not detected
Collagen-dish	156.7 ± 3.1†	119.3 ± 6.0	15.5 ± 2.9

The cell number and the alkaline phosphatase activities were expressed as a ratio of against those on gold-coated coverslip. Both the alkaline phosphatase activities and the calcium amounts were normalized by the cell number.

* $p < 0.05$ against "Gold" and SAM-COOH group, and $p < 0.01$ against other SAM.

** $p < 0.05$ against "Gold."

† $p < 0.01$ against all other groups.

cultured on prepared SAM surfaces (Table II). When NHOsts were cultured on SAM-CH_3 surface, not only the cell number but also their ALP activity decreased and the amounts of deposited calcium per cell were not detected. This suggests that NHOsts cannot maintain their differentiation level when they cannot adhere on the surface. When NHOsts were cultured on SAM-OH, SAM-COOH, or SAM-NH_2, their number, ALP activity and deposited calcium amounts per cell were almost the same as those observed on a gold surface. These indicate that a surface property that affects cell adhesion level is a one of factors to regulate differentiation level of NHOst. Interestingly, when NHOsts were cultured on SAM-OPO_3H_2 or SAM-OSO_3H, ALP activity of NHOsts and the amounts of calcium deposition per cell increased although the cell number ratio was about a one-third to a half of that observed on a gold surface. Tanahashi and Matsuda have reported that a surface covered with negatively charged chemical groups enhances the growth rate of apatite when it was soaked in a simulated body fluid because of interaction between calcium ion and the surface.[23] Interestingly, an apatite growth rate on SAM-OPO_3H_2 has been reported to be higher than that on SAM-COOH,[23] suggesting an equilibrium constant of the functional groups, which determines their negative charge level in physiological pH, affects strength of the interaction. In this study, SAM-COOH cultured with NHOsts showed almost the same calcium deposition as SAM-OH and gold surface, while SAM-OPO_3H_2 and SAM-OSO_3H showed calcium deposition 4 to 7 times as much as other surfaces tested. In addition, ALP activity of NHOsts on these two SAM surfaces was higher than any other surfaces including collagen-coated dish, which is normally utilized for a culture of NHOsts. Table I indicates that contact angle of SAM-OH is almost similar to that of SAM-OSO_3H and there are no statistical differences among contact angles of 3 SAMs, SAM-OSO_3H, SAM-COOH, and SAM-OPO_3H_2. Therefore, these findings suggest that chemical composition of the surfaces, which determines its ionic charge and zeta potentials of surfaces in physiological pH, may be one of key factors to regulate differentiation level of osteoblasts more than their hydrophilic/hydrophobic balance. As different ionic charge of SAM surfaces has been reported to influence protein adsorption as well as their hydrophilic/hydrophobic balances,[36] it is necessary to evaluate actual zeta potentials of prepared SAM surfaces in physiological pH before investigating the interaction between various functional groups and proteins including vitronectin and fibronectin, which may provide valuable information of effects of the functional groups on the cell differentiation level as well.

Although the differentiation level of NHOsts was influenced by the functional groups on SAM surfaces, their GJIC level after 1-day culture were almost the same as that of NHOsts cultured on a collagen-coated dish as a control experiment, irrespective of the type of functional group (Table III). This indicates that NHOsts interacting with these functional groups can maintain their homeostasis, irrespective of the kind of the functional group. Although GJIC has been reported to play a role in differentiation of osteoblasts,[37,38] the effect of the functional group on differentiation level of NHOsts observed in this study may be

TABLE III. Gap Junctional Intercellular Communication Activity of NHOst on Various SAM Surfaces after 1-day Incubation Measured by FRAP Analysis Technique

	Collagen-Coated Dish (control)	Gold	SAMs Modifying Surfaces					
			SAM-OH	SAM-OSO_3H	SAM-COOH	SAM-OPO_3H_2	SAM-NH_2	SAM-CH_3
GJIC activity (Ratio vs. control)	1.00 ± 0.38	1.00 ± 0.69	1.11 ± 0.46	0.92 ± 0.47	0.87 ± 0.41	1.12 ± 0.41	1.15 ± 0.46	1.24 ± 0.54

All values were calculated as a ratio of the activity against that obtained from NHOsts on a collagen-coated culture dish (control). (n = 12–14).